WOODHEAD PUBLISHING SERIES IN ELECTRONIC AND OPTICAL MATERIALS

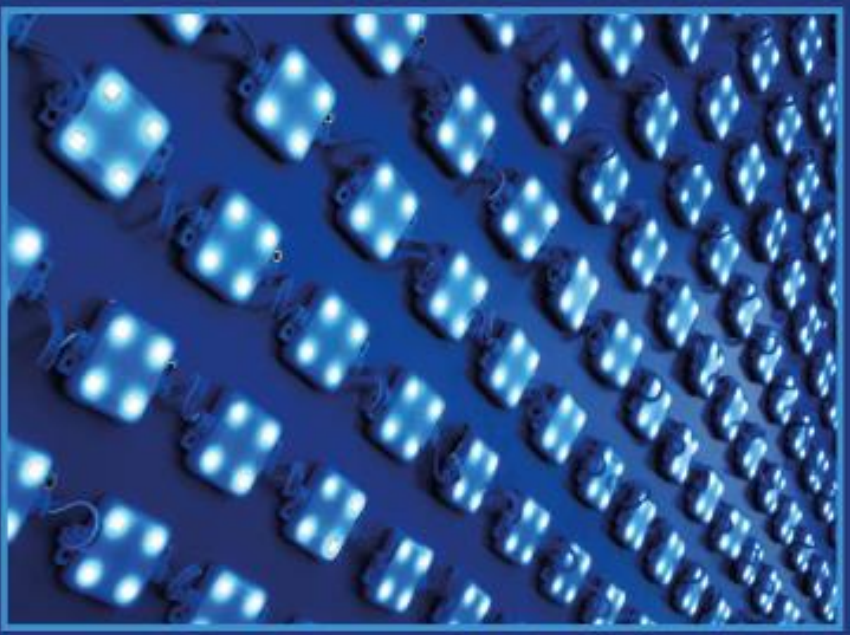

FUNCTIONAL MATERIALS FROM CARBON, INORGANIC, AND ORGANIC SOURCES

METHODS AND ADVANCES

Edited by
SANJAY J. DHOBLE, AMOL NANDE,
N. THEJO KALYANI, ASHISH TIWARI,
ABDUL KARIEM AROF

ELSEVIER

Woodhead Publishing Series in Electronic and Optical Materials

Functional Materials from Carbon, Inorganic, and Organic Sources

Methods and Advances

Edited by

Sanjay J. Dhoble
Amol Nande
N. Thejo Kalyani
Ashish Tiwari
Abdul Kariem Arof

WP
WOODHEAD PUBLISHING
ELSEVIER An imprint of Elsevier

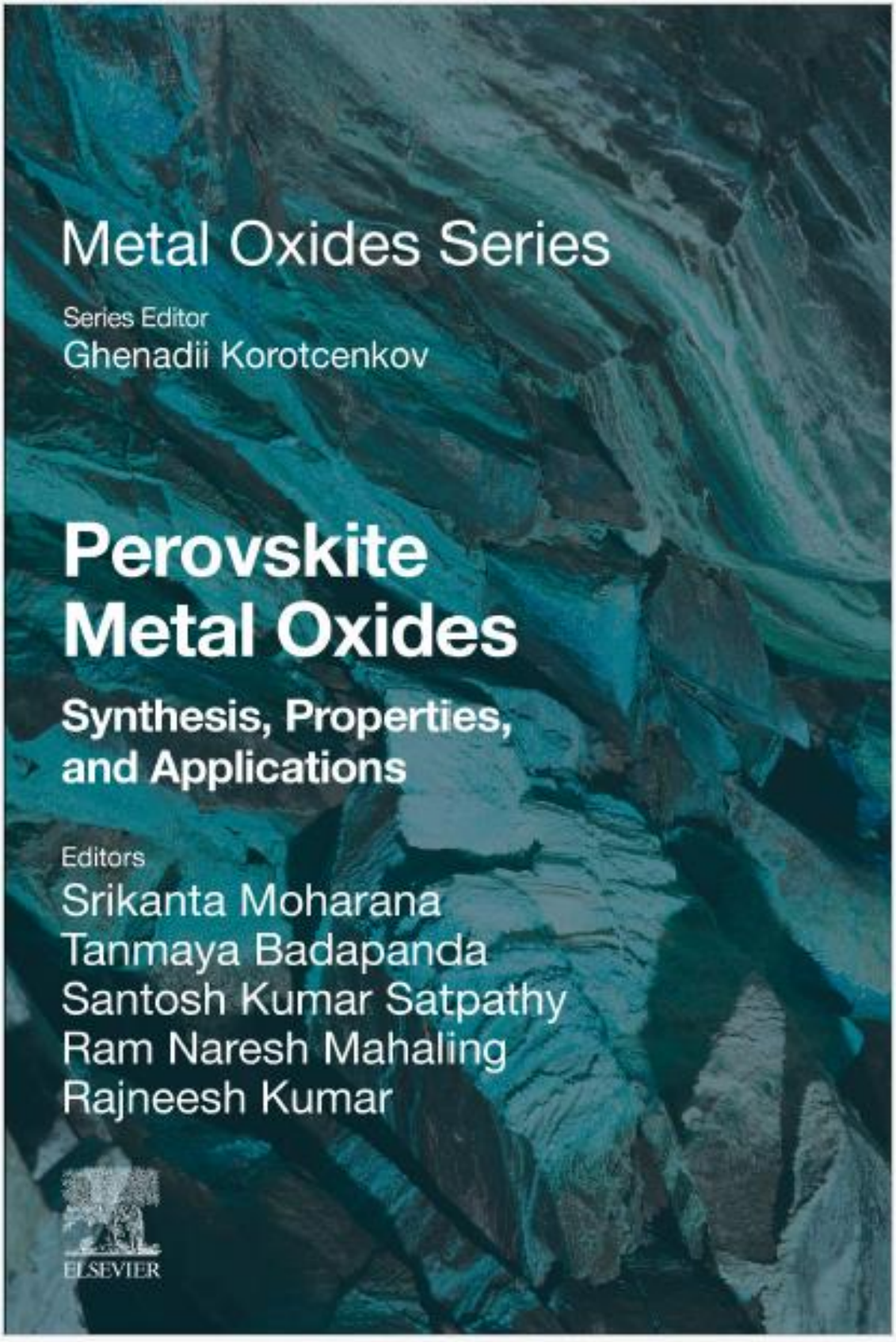
Metal Oxides Series
Series Editor
Ghenadii Korotcenkov
Perovskite Metal Oxides
Synthesis, Properties, and Applications
Editors
Srikanta Moharana
Tanmaya Badapanda
Santosh Kumar Satpathy
Ram Naresh Mahaling
Rajneesh Kumar
ELSEVIER

Metal Oxides

Perovskite Metal Oxides

Synthesis, Properties, and Applications

Edited by

Srikanta Moharana

Department of Chemistry, School of Applied Sciences, Centurion University of Technology and Management, Bhubaneswar, Odisha, India

Tanmaya Badapanda

Department of Physics, C.V. Raman Global University, Bhubaneswar, Odisha, India

Santosh Kumar Satpathy

Department of Physics, School of Applied Sciences, Centurion University of Technology and Management, Bhubaneswar, Odisha, India

Ram Naresh Mahaling

School of Chemistry, Sambalpur University, Jyoti Vihar, Burla, Sambalpur, Odisha, India

Rajneesh Kumar

Department of Physics, Institute of Science, Banaras Hindu University, Varanasi, Uttar Pradesh, India

Series Editor

Ghenadii Korotcenkov

Department of Physics and Engineering, Moldova State University, Chisinau, Republic of Moldova

IOP Conference Series: Materials Science and Engineering

Oxygen vacancy related conduction behavior in $BaZr_{0.05}Ti_{0.95}O_3$ ceramic

IOP Conf. Series: Materials Science and Engineering **798** (2020) 012006 doi:10.1088/1757-899X/798/1/012006

Oxygen vacancy related conduction behavior in $BaZr_{0.05}Ti_{0.95}O_3$ ceramic

G. Nag Bhargavi[1], Tanmaya Badapanda[2], Ayush Khare[3], M. Shahid Anwar[4] and Nameeta Brahme[5]

[1]*Department of Physics, Govt. Pt. Shyamacharan Shukla College Dharsiwa Raipur- 493221, India*
[2]*Nanophotonics Laboratory, Department of Physics, C.V. Raman College of Engineering, Bhubaneswar-752054, India*
[3]*Department of Physics, National Institute of Technology, Raipur-492010, India,*
[4]*Colloids & Materials Chemistry, Institute of Minerals and Materials Technology, Bhubaneswar-751013, India*
[5]*School of Studies in Physics and Astrophysics, Pt. Ravishankar Shukla University, Raipur-492010, India*

Abstract. For this study, the microcrystalline powder of $BaZr_{0.05}Ti_{0.95}O_3$ (BZT) was prepared by the conventional solid state reaction method. The sample was calcined at 1200 °C for 4 hours and sintered at 1300 °C. The calcined powder was structurally characterized by X-ray diffraction (XRD), which showed that the specimen has a Perovskite structure having orthorhombic structure. On analyzing the scanning electron microscope (SEM) the calculated crystal size was observed to range between 20- 30 μm. The dielectric study of BZT showed normal phase transition behavior. The conductivity studies as a function of temperature and frequency has been performed to study the role of oxygen vacancies. The results of the frequency dependence of the conductivity suggest that oxygen vacancy hopping processes, due to relaxations in oxygen vacancy-related dipoles, being mainly responsible for the conduction behavior in the studied system.

Keywords: Solid state reaction method, XRD, SEM, Dielectric study, Conductivity

1. Introduction

Barium titanate (BT) is a well known Perovskite structured material, which is known for its high dielectric constant, spontaneous polarization, ferroelectric properties and non linear optical properties. It is given in the open literature that the properties of BT can be enhanced by the substitution at Barium and/or Titanium sites by homovalent or aliovalent ions [1-6]. This lead (Pb) free compound has numerous applications in DRAMs, MLCCs, ultra sonic transducers, optical data storage at high density, sensors, actuators and optoelectronic devices [7-9]. Among the homovalent substituents Zr^{4+} in place of Ti^{4+} has been reported to improve the dielectric properties of BT [10-12]. This ceramic with general formula $BaZr_xTi_{1-x}O3$ shows promising piezoelectric and electrostrictive properties [13, 14]. Better thermal and chemical stability of Zr^{4+} than Ti^{4+} makes Zr^{4+} a best choice as isovalent substituent for substitution at Ti sites [15]. Also, the ionic radius of Zr^{4+} (0.087 nm) is larger than Ti^{4+} (0.068 nm) which expand the unit cell and the possibility of electron hopping between Ti^{4+} ions and Ti^{3+} ions reduces to a large extent [15].

In case of all the oxide Perovskites the oxygen vacancies are the fundamental intrinsic defects that play a very critical impact on the electrical properties. The oxygen vacancies do not lost

their identity even after the process of sintering. In all the oxide ferroelectric materials the dielectric relaxation is usually related to the vacancies produced at oxygen sites. It is extensively accepted that the dielectric relaxation in oxide materials specifically at high temperatures are usually related to oxygen vacancies, apart from this dielectric relaxation appear in the low-frequency region is also attributed to oxygen-vacancies [16, 17]. So, it is very interesting to study the conduction behavior of BZT system in terms of oxygen vacancies.

The material performances are closely dependent on the methods of synthesis. In case of ferroelectric ceramics the method of synthesis is prominent in determining the various structural and electrical properties. There are various methods of synthesis like solid state reaction method, ball milling, wet chemical synthesis, combustion technique, Sol-gel technique etc. [18-20]. Among these some are chemical routes while some are physical (high temperature diffusion) routes. In the present work, we have chosen the high temperature solid state reaction methods. The chemical routes of processing require costly chemicals which are very sensitive to the environment and physical conditions like light heat and moisture. On the other hand the solid state reaction method uses carbonates and oxides which are easily available and also cost effective.

So, in this study the main objective of the authors is to synthesize $BaZr_{0.05}Ti_{0.95}O_3$ ceramic system by the conventional solid state reaction method and to study in detail the electrical conduction behavior in terms of oxygen vacancies.

2. Experimental Procedure

The sample ($BaZr_{0.05}Ti_{0.95}O_3$) was synthesized by the traditional solid state reaction method. The stoichiometric mixture of powders ($BaCO_3$, TiO_2, ZrO_2) was mixed and grinded in an agate mortar with a little amount of distilled water. The mixture was fired at 1200 ℃ for calcination for 4 hours in a high temperature furnace. The chemical reaction for the above process is shown in eq. (1). The Perovskite phase structure of the sample was confirmed under the X-ray diffraction analysis (X'pertPro Diffractometer). The analyzed 2θ range was 10°-90° with a step rate of 0.02° and counting time of 0.5 minute for each step. The microstructure of the sintered sample was observed by scanning electron microscope (Zeiss EVO 18). The fired powder was formed as a thick disc (1mm) by cold pressing and sintering was carried out at 1300 ℃ for 4 hours. The sintered disc was polished with silver paint to make the surface conducting to carry out the electric studies (N4L-NumeriQ LCR meter, Model PSM 1735).

$$BaCO_3 + 0.05ZrO_2 + 0.95TiO_2 \rightarrow BaZr_{0.05}Ti_{0.95}O_3 + CO_2 \uparrow \quad (1)$$

3. Results and Discussion

3.1 *Structural Characterization*

Fig. 1 is presenting the XRD pattern of $BaZr_{0.05}Ti_{0.95}O_3$ system which is calcined at 1200 ℃ for 4 hours. The X- ray diffraction pattern could be indexed as a pure Perovskite structure. No impurity peak corresponding to any deleterious phase was found which confirms the single phase nature of the compound. Moreover, the sharp intense and well defined diffraction peaks indicate that the ceramic material has a long range degree of crystallinity. The obtained

phase was indexed using the orthorhombic space group *Amm2* which is in close agreement with the earlier reports [15, 21].

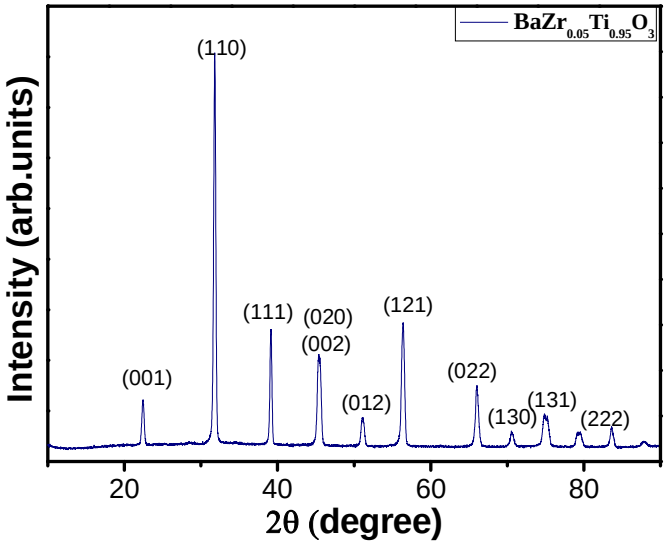

Fig. 1 XRD pattern of $BaZr_{0.05}Ti_{0.95}O_3$ ceramic

3.2 *Microstructural studies*

Fig. 2(a) shows the morphological image of $BaZr_{0.05}Ti_{0.95}O_3$ ceramic pellet sintered at 1300 °C taken from SEM. The SEM investigation has shown that the microstructures of the specimen exhibit a good growth of grains. The image showed that the grains are in irregular polygon shape. Also the grains developed with irregular morphology have multiple grain boundaries. This characteristic is mainly attributed to the matter transportation mechanism at high temperatures during the solid state reaction. Also, the average crystallite size is estimated by line intercept method which is observed to be 20- 30 μm. The compositional characterization of $BaZr_{0.05}Ti_{0.95}O_3$ ceramic sintered at 1300 °C was also done using Energy dispersive X-ray spectroscopy (EDX) which is shown in fig. 2(b). The measurements were taken at different locations and then averaged. Table 1 shows the calculated and EDX derived composition of $BaZr_{0.05}Ti_{0.95}O_3$ ceramic. There exist small variation in both the data which possibly due the deficiency of oxygen during sintering at high temperature. Moreover, in solid state reaction method it is always difficult to get the microscopic uniformity.

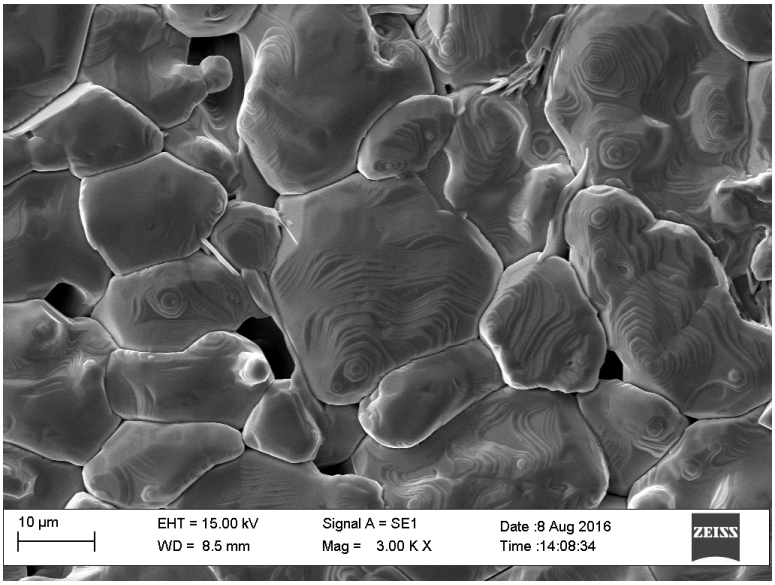

Fig. 2(a) SEM image of $BaZr_{0.05}Ti_{0.95}O_3$ ceramic sintered at 1300 °C

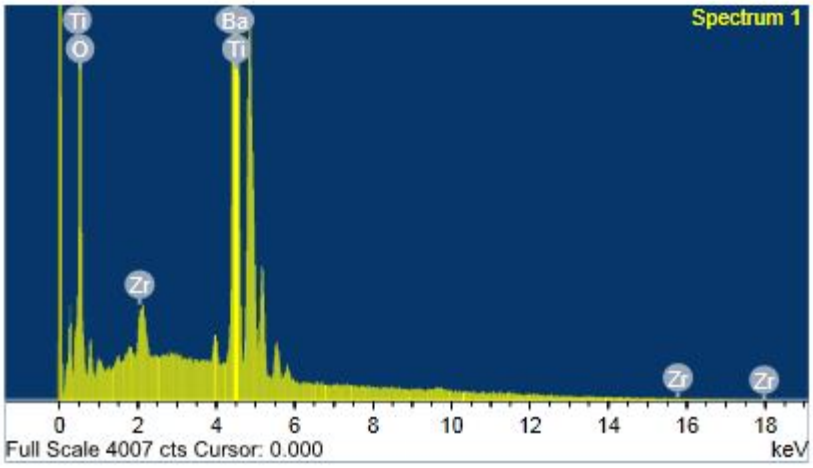

Fig. 2(b) EDX spectrum showing the elemental composition of $BaZr_{0.05}Ti_{0.95}O_3$ ceramic

Table 1 Calculated and EDX derived composition of $BaZr_{0.05}Ti_{0.95}O_3$ ceramic

Element	Wt.% calculated	Wt.% from EDX
Ba	57.59	57.65
Zr	1.48	1.59
Ti	18.52	18.12
O	22.41	22.64

3.3 The Ferroelectric – Paraelectric phase transition

Fig. 3 depicts the change in inverse of permittivity ($1/\varepsilon'$) as a function of temperature performed at 100 kHz. It is known that for normal ferroelectrics the ferro- to – paraelectric

phase transition is known to be first order when $T_0 < T_c$ and of second order when $T_c=T_0$, here T_c is the Curie-Weiss temperature which is defined by the following relation:

$$\frac{1}{\varepsilon_r} = \frac{T-T_C}{C} \quad (2)$$

Curie - Weiss law is no longer valid in the case where relaxation and diffuseness are present. For all the relaxor ferroelectrics (having diffuse phase transition) a deviation from Curie – Weiss law is observed which is a typical behavior of relaxors. The parameter $\Delta T_m = T_{CW} - T_m$, where T_{CW} denotes that temperature from which the dielectric permittivity starts to deviate from the Curie - Weiss law while T_m is the temperature of dielectric maximum. In the present study for $BaZr_{0.05}Ti_{0.95}O_3$ the phase transition was observed to be first order i.e. no deviation from ideal Curie Weiss law is observed. Also, the phase transition temperature was measured to be 400 K.

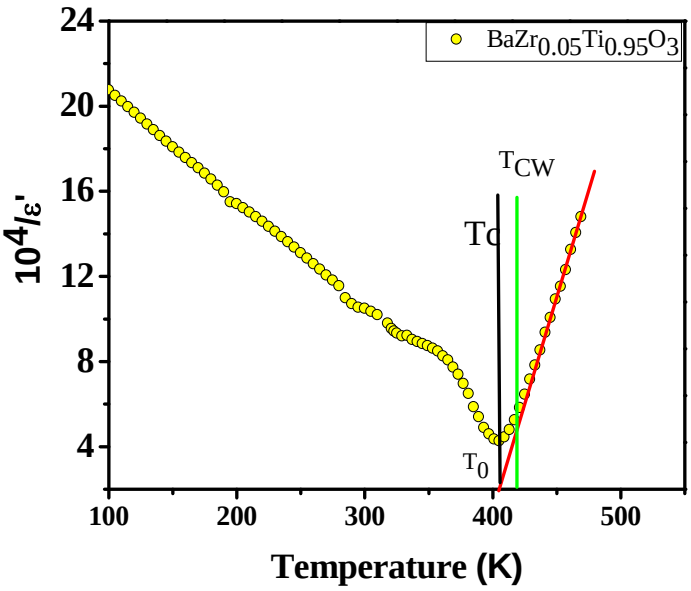

Fig. 3 Change in 1/ε′ with respect to temperature measured at 1 kHz

3.4 AC Conductivity in ferroelectric phase

Fig. 4 shows the variation of AC conductivity of $BaZr_{0.05}Ti_{0.95}O_3$ with reciprocal of temperature (10^3/T) measured at 1 KHz. The observed variation in AC conductivity with temperature could be divided into two distinct regions in the scale namely the lower temperature region and the higher temperature region. Being activated by the various temperatures the oxygen vacancies behaves as trapping centres for the mobile charge carriers. Also an increase in the conductivity considerably in the high temperature region is seen probably this is due to the hopping of the charge carriers among the available oxygen vacancies. Another important fact we observed from the graph is the changing slopes that appear in different regions of temperature scale, which is an indication of involvement of multiple activation processes having different activation energies. The AC conductivity first

increases with temperature up to 125 °C and then decreases with increasing in temperature, which also represents the transition temperature.

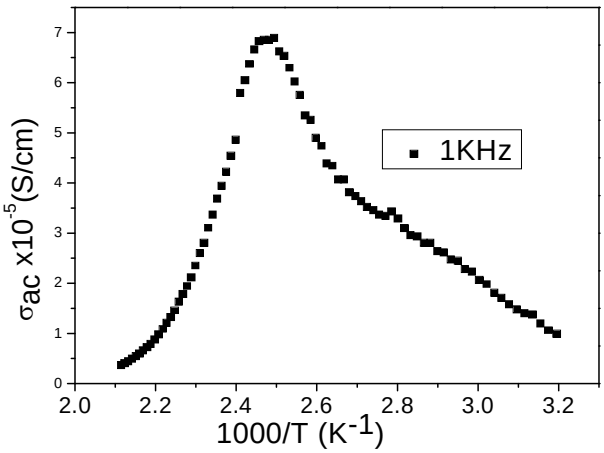

Fig. 4 AC conductivity of BZT ceramic plotted against 1000/T measured at 1 kHz

In all the dielectric materials there exist several polarization mechanisms; these mechanisms have some relationships with the relaxation behaviour like space charge polarization, interfacial polarization, dipolar polarization etc. The dielectric relaxation due to space charge polarization, interfacial polarization, domain wall motion, long range structural disorder and defect relaxation etc. usually occurs at low frequency region while the dipolar relaxation occurs at higher frequency region. It is given in the open literature that the dielectric relaxation in all the dielectric materials in the temperature above room temperature is usually related to the available oxygen vacancies and hopping motion of singly and doubly ionized oxygen vacancies leads to the relaxation process.

Thus, it can be considered that in the low frequency spectral region the relaxation belongs to space charge that is related to the oxygen vacancies and the defect sites. While sintering at high temperatures produces Barium vacancies which results in oxygen vacancies due to the constraints of charge neutrality. At high temperatures the ionization of oxygen vacancies takes place that create conducting electrons in the Perovskite structure as a result single ionized and double ionized oxygen vacancies are left where $V_O^{'}$ and $V_O^{''}$ are respectively the single ionised and double ionised states. Thus, as described by the Kroger -Vink notation:

$$V_O \leftrightarrow V_O^{'} + e^{'} \quad (3)$$

$$V_O^{'} \leftrightarrow V_O^{''} + e^{'} \quad (4)$$

$$Ba_{Ba}^{x} + O_O^{x} \rightarrow V_{Ba}^{''} + V_O^{''} + BaO \uparrow \quad (5)$$

Further to understand the transport mechanism in the samples the electrical conductivity behavior was investigated. The transport mechanism is basically due to the presence of space charge in the material. The origin of conductivity mechanism is related to the level and mobility of oxygen vacancies which is a common phenomenon in perovskites. As it is known the AC conductivity of the samples is directly related to the dielectric properties of the sample. To evaluate the bulk conductivity (σ_{ac}) of the samples the formula used is $\sigma_{ac} = t/Z'A$ where t is the thickness, A is the surface area of the samples and Z′ is the real part of the

impedance. Fig. 5(a) indicates the ac conductivity of the $BaZr_{0.05}Ti_{0.95}O_3$ samples at various frequencies (from RT to T_c). Initially, with increasing frequency, σ is almost independent of frequency followed by dispersion at higher frequencies. By extrapolating the graph towards lower frequency side the value of σ_{dc} can be determined which is credited to the long range translational motion of charge carriers. It is also observed that with increasing temperature conductivity increases for all frequencies. Conduction in perovskites is basically due to the hopping mechanism of different species of ions present in the material. The excess electrons interact with the lattice and distort the surroundings as a result a potential well is created which raise the conduction. As the temperature increases the number of excess electrons increases and get sufficient energy to cross the well, thus with increasing temperature conductivity increases. The change in AC conductivity in the lower frequency region is mainly due to the polarization effect at electrode and electrolyte interface. At much lower frequencies the charge accumulates at the electrode and electrolyte interface and reduces the conductivity almost equal to the DC conductivity. At higher frequencies the characteristic of conductivity spectra can be explained as according to the Jonscher's power law. According to which $\sigma_{ac} = \sigma_{dc} + A\omega^n$ $(0 < n < 1)$ where, A is the pre-exponential factor and 'n' is the exponent of power law which gives the idea of interaction between mobile ions and lattice. 'A' gives the idea of strength of polarizability in the samples.

The variation of AC conductivity with respect to inverse of temperature by means of Arrhenius law is shown in fig. 5(b). The slope of this graph determines the value of activation energy involved in the conduction process. Conduction induced by oxygen vacancies becomes dominant with increasing temperature because the mobility of oxygen ions becomes higher in high temperature region. It has been reported in the literature that the when the activation energy lies in the range of 0.3-0.4eV, the oxygen vacancies lies in the single ionized state while for the doubly ionized oxygen vacancies the value lies between 0.6-1.2eV. The experimental value of activation energy associated with the DC conductivity for the studied sample is 1.1eV. The results are in good agreement with the values reported for the doubly ionized oxygen vacancies.

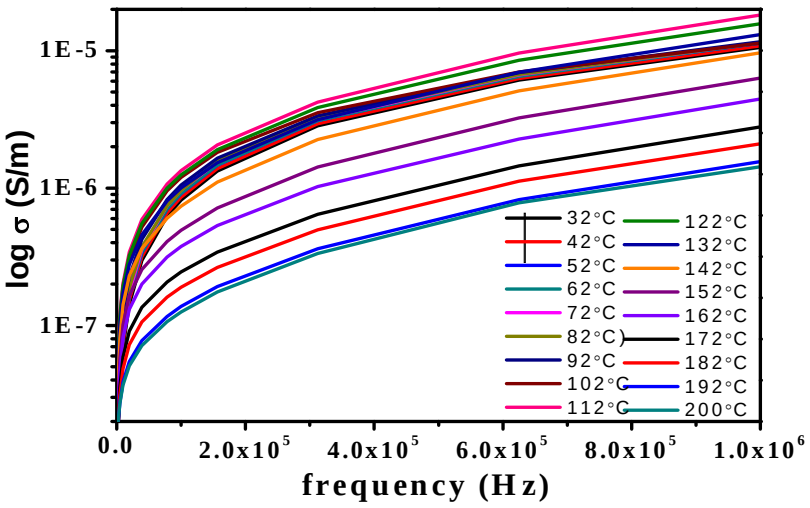

Fig. 5(a) AC conductivity as a function of frequency at various temperatures

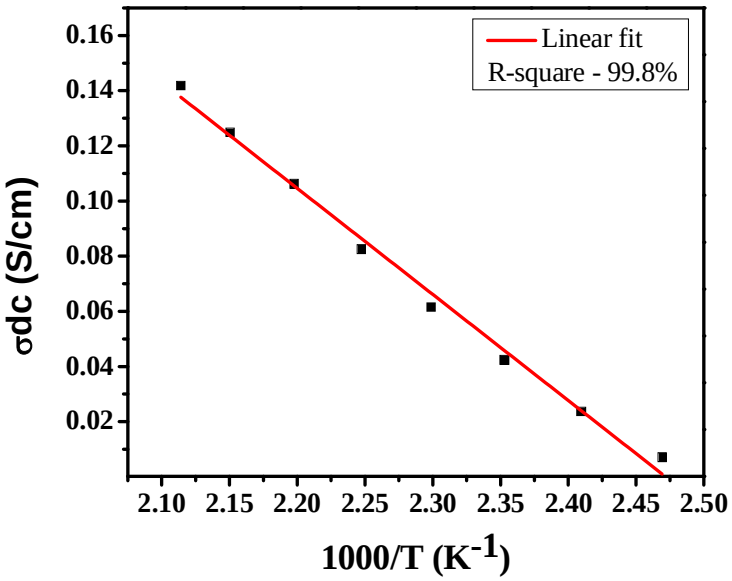

Fig. 5(b) Arrhenius dependence for dc conductivity as a function of 1000/T (K^{-1})

4 Conclusions

Thus, we conclude that polycrystalline sample of $BaZr_{0.05}Ti_{0.95}O_3$ ceramic has been synthesized by the high temperature solid state reaction method. The X-ray diffraction studies revealed the presence of orthorhombic phase. The dielectric measurements of $BaZr_{0.05}Ti_{0.95}O_3$ ceramic with respect to temperature at 1 kHz has been analyzed, no deviation from Curie – Weiss law has been seen indicating the normal ferroelectric phase transition in the sample. The studies show that the conduction was caused by the presence of oxygen vacancies. Also, the dielectric relaxation at high temperature was related to the presence of oxygen vacancies.

References

[1] Belous A G, V'yunov O and Khomenko B S 1998 *Inorg. Mater.* 34(6) 725-729
[2] Bąk W, Kajtoch C, Ptaszek S, Lisińska-Czekaj A, Czekaj D, Ziętek D, Glos T and Garbarz-Glos B 2016 *Arch. Metall. Mater.* 61(2) 905–908

[3] Guo Z G, Yang L, Qiu H, Zhan X, Yin J and Cao L 2012 *Mod. Phys. Lett. B* 26(9) 1250056

[4] Slipenyuk A M, Glinchuk M D, Bykov I P, Yurchenko L P, Mikheev V A, Frenkel O A, Tkachenko V D and Garmash E P 2003 *Cond. Mat. Phys.* 6 2(34) 237-244

[5] Wang Y, Pu Y and Zhang P 2015 *J. Alloys Compds.* 653(25) 596-603

[6] Lyu J, Fina I, Solanas R, Fontcuberta J and Sánchez F 2018 *Scientific Reports* 8 495 DOI:10.1038/s41598-017-18842-5.

[7] Ertuğ B 2013 *Amer. J. Eng. Resear* 02(08) 01-07

[8] Wu L, Chure M C, Wu K, Chang W C, Yang M J, Liu W K and Wu M J 2009 *Ceram. Int.* 35(3) 957-960

[9] Jiang B, Iocozzia J, Zhao L, Lin Z, Zhang H, Harn Y W and Chen Y 2019 *Chem. Soc. Rev.* 48(4) DOI: 10.1039/C8CS00583D.

[10] Kumar R, Asokan K, Patnaik S and Birajdar B 2015 *DAE Sol. Stat. Phys. Symposium AIP Conf. Proc.* 1731 030025-1–030025-3; DOI: 10.1063/1.4947630.

[11] Feng H, Hou J, Qu Y, Yao G and Shan D 2012 *J. Alloys Compds*. 512(1) 12–16

[12] Kheyrdan A, Abdizadeh H, Shakeri A and Golobostanfard M R 2018 *J. Sol-Gel Sci. Tech.* 86(1) 141–150

[13] Rehrig P W, Park S E, McKinstry S T, Messing G L, Jones B and Shrout T R 1999 *J, Appl.Phys.* 86(3) 1657

[14] Wieczorek K, Ziebiniska A, Ujma Z and Roleder K 2006 *Ferroelect.* 336(1) DOI: 10.1080/00150190600695743.

[15] Bhargavi G N, Khare A, Badapanda T, Anwar M S and Brahme N 2017 *J. Mater. Sci.: Mater. Electron.* 2816956–16964 DOI 10.1007/s10854-017-7617-8

[16] Barranco A P, Guerra J D S, Noda R L and Araujo E B 2008 *J. Phys. D: Appl. Phys.* 41 215503

[17] Zhang T F, Tang X G, Liu Q X, Lu S G, Jiang Y P, Huang X X and Zhou Q F 2014 *AIP Advances* 4 107141

[18] Badapanda T, Sarangi S, Behera B, Sahoo P K, Anwar S, Sinha T P, Luz Jr. G E, Longo E and Cavalcante L S 2014 *Curr. Appl. Phys.* 14 708-715

[19] Dixit A, Majumder S B, Savvinov A, Katiyar R S, Guo R and Bhalla A S 2002 Mater. Letts. 56 933 – 940

[20] Ahmad A and Razak K A 2017 *AIP Conf. Proc.* 1865 060001 DOI.org/10.1063/1.4993377

[21] Bhargavi G N, Khare A, Badapanda T, Ray P K and Brahme N 2018 *Ceram. Int.* 44 1817–1825

IOP Conference Series: Materials Science and Engineering

A study of enhanced structural, microstructural and dielectric behaviour of aliovalent ions doped $BaZr_{0.05}Ti_{0.95}O_3$ ceramic

A study of enhanced structural, microstructural and dielectric behaviour of aliovalent ions doped $BaZr_{0.05}Ti_{0.95}O_3$ ceramic

G Nag Bhargavi[1], Tanmaya Badapanda[2], Ayush Khare[3] and M Shahid Anwar[4]

[1] Department of Physics, Govt. Pt. Shyamacharan Shukla College Dharsiwa Raipur-493221, India
[2] Nanophotonics Laboratory, Department of Physics, C.V. Raman College of Engineering, Bhubaneswar-752054, India
[3] Department of Physics, National Institute of Technology, Raipur-492010, India,
[4] Colloids & Materials Chemistry, Institute of Minerals and Materials Technology, Bhubaneswar-751013, India

*Corresponding author's e-mail address: bhargavi.nag24@gmail.com

Abstract. The lead-free ceramics are considered to be the best substitutes for lead based ceramics which have tremendous harmful effects regarding environmental pollution. In this concern, the lead-free ceramics have been widely attracted by research communities. In the present study we have prepared lead free $BaZr_{0.05}Ti_{0.95}O_3$perovskite ceramics with various doping concentrations of Gd^{3+} ions by the conventional solid-state reaction method. The perovskite phase formation was studied by x-ray diffraction which indicate the transformation of crystal symmetry from orthorhombic to tetragonal structure for the Gd^{3+} ions doped samples. The scanning electron microscopy studies revealed the modification in grain size on doping Gd ions also the energy dispersive X-ray spectra have been obtained to study the compositional variations. The dielectric and loss studies have been performed in the large range of temperature and frequency. The low dielectric loss and high dielectric constant suggests possible applications in memory devices and ceramic capacitors. Temperature coefficient of capacitance plots have also been plotted.

1. Introduction

$BaTiO_3$(BT) a commonly known perovskite was commercially used for acoustic and ultrasonic generation and detection though its Curie temperature was quite low (i.e. 120 °C) [1-6]. Soon it was replaced by another perovskites like $PbTiO_3$ and Pb(Zr, Ti)O_3 [7-13]. Though the lead based ceramic compounds have proved to be extremely good as far as the industrial needs are concerned but, the toxicity of Pb restricts its practical applications. Thus, in recent years the need for lead free perovskite ceramics caused a reconsidered interest in $BaTiO_3$ based ceramics [14-18]. The structural and dielectric properties of $BaTiO_3$ can be modified to a large extent by the addition of some aliovalent ions (heterovalent dopants) such as La^{3+}, Ce^{3+}, Nb^{5+}, Nd^{3+}, Pr^{3+}, Eu^{3+}, Er^{3+}, Gd^{3+}, Mg^{2+}, Sn^{4+} etc. on Ba^{2+} or Zr^{4+} on Ti^{4+} sites that forms the solid solution [19-26]. Among various compositions Zr^{4+} with ~15% substitution in Ba(Zr, Ti)O_3(BZT) undergoes three structural phase transitions (rhombohedra to orthorhombic, orthorhombic to tetragonal and tetragonal to cubic) like $BaTiO_3$, also the Curie temperature decreases [27-30]. After thorough investigation of literature, out of the several rare earth ions our focus was on Gd whose ionic radius is 0.91Å. The incorporation of rare-earth (Gd^{3+}) ions into

the BT host system was studied by Borah et al. in 2014 [31]. The results of their study revealed that Gd^{3+} ions greatly manifest dielectric relaxation and carrier conduction mechanisms. The dielectric constant showed a decreasing trend with doping content and with increasing frequency. However, in the low-frequency region due to the combined result of orientational polarization and electrical conduction the loss tangent (tan δ), was found to be quite high in the doped samples as compared to their un-doped counterpart. In another study the amphoteric nature of Gd^{3+} ions were discussed by Li et al.in 2012 [32]. According to the study because of the mediocre ionic radius of Gd^{3+} ion, it may replace the A-site ions or B-site ions. After the analysis of XRD patterns they revealed that different substitution sites of Gd^{3+} ions could be affected by amount of Gd_2O_3 doping. Gd^{3+} tended to occupy Ba-site when Gd_2O_3 concentration was less than 0.25 mol%. On further increasing concentration of Gd_2O_3 doping amount to 0.3 mol%, Gd^{3+}ions get substituted into both the Ba- and Ti-sites as a result of which an improvement on dielectric constant of $BaTiO_3$-based ceramics is seen. They used self-compensation model to discuss the dielectric behaviour. Reddy et al. in 2011[33] gave a detailed study of dielectric studies properties when Gd^{3+} ions are doped at A site of $BaZr_{0.1}Ti_{0.9}O_3$ ceramic. The microstructural investigation on the sintered ceramics showed that Gd doping significantly reduced the grain size of pure BZT ceramics. Change in the Gd concentration had minor influence on the grain size and on morphology. The Curie temperature (T_C) significantly decrease with an increase in the Gd content. However, the maximum value of dielectric constant at T_C was seen for 2 mol% Gd and on further increase in Gd content the dielectric constant at T_C decreased. They reported that the dielectric constant was significantly improved as compared to that of undoped BZT ceramic. Hence it is concluded that the tunable dielectric materials with good dielectric properties can be prepared by doping BZT with Gd.

In the present study we have chosen 5 mole % Zr^{4+} doped BT i.e. $BaZr_{0.05}Ti_{0.95}O_3$ as base material. This composition of BZT shows normal ferroelectric behavior and also the presence of morphotropic phase boundaries give special features by improving the piezoelectric properties. Further we have chosen Gd^{3+} as an heterovalent ion which can replace Ba^{2+} ions at A-site as according to the formula $Ba_{1-x}Gd_{2x/3}Zr_{0.05}Ti_{0.95}O_3$. Thus, the objective of the present work is to study the influence of Gd^{3+} ions doping on the dielectric properties of $BaZr_{0.05}Ti_{0.95}O_3$.

2. Materials and methods

The perovskite samples of pure and Gd doped Barium Gadolinium Zirconium Titanate with formula $Ba_{1-x}Gd_{2x/3}Zr_{0.05}Ti_{0.95}O_3$ (x=0.00, 0.01, 0.02) were prepared by conventional high temperature solid state reaction method. For the sake of convenience, we will mention the samples as BZT, BGZT1 and BGZT2 for x= 0.00, 0.01 and 0.02 respectively. The starting raw materials were $BaCO_3$, TiO_2, ZrO_2 and Gd_2O_3 (all from Merck India) all were more than 99% pure. The stoichiometric ratio of all the chemicals were thoroughly mixed in an agate mortar in dry and wet mixing with appropriate amount of Acetone for 5 hours. After proper mixing the samples were calcined at 1200℃ for 4 hours at a heating rate of 5 ℃ per minute. A small amount of polyvinyl alcohol was added to the calcinated powders for the fabrication of pellets which were sintered at 1250 ℃. The circular disc shaped pellets were prepared by applying uniaxially a pressure of 200 MPa. A preliminary study on compound formation and structural parameters was carried out using an X-ray diffraction (XRD) technique with an X-ray powder diffractometer. The XRD pattern of the calcinated powder was recorded at room temperature PANAlytical X'pert pro with Cu-K_α radiation (1.5405 Å) in a wide range of Bragg's angles 2θ ($20 \leq 2\theta \leq 80$). The dielectric constant and dielectric loss were measured on N4L-NumetriQ LCR meter (model PSM1735).

3. Results and Discussions

3.1 Structural characterization

The X-ray diffraction patterns of BZT, BGZT1 and BGZT2 ceramic specimen are shown in figure1. After a keen analysis by X'pert Highscore software, the Perovskite structure was identified for all the specimens at room temperature. The peaks of BGZT1 and BGZT2 specimens seems to move slightly towards right (higher 2θ). The lattice parameters from the XRD data were calculated using Checkcell

software shown in inset. The structural evolution of the specimens with these compositional changes can be readily understood in terms of the ionic radii of the cations at A-site (r_{Ba2+} = 1.61 Å and r_{Gd3+} = 0.91Å) and B-site (r_{Ti4+} = 0.605 Å and r_{Zr4+} = 0.72 Å). The splitting of peaks at 2θ=45˚ for BGZT1 and BGZT2 show the tetragonal symmetry indicating the ferroelectric phase at room temperature. However, for the BZT sample the crystal symmetry was observed to be orthorhombic at room temperature. The inset shows the variation of d-spacing and cell volume both these values decrease with increasing concentration of Gd.

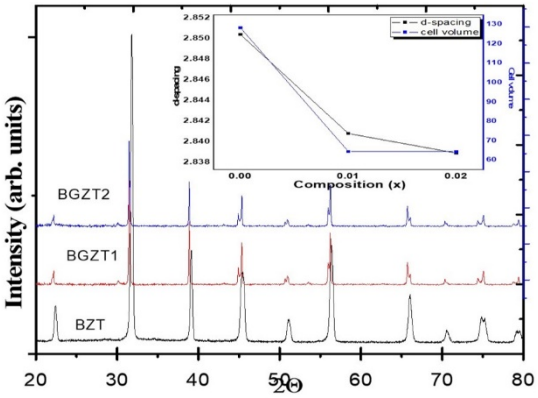

Figure 1. XRD plots of BZT, BGZT1 and BGZT2 at room temperature. The inset is variation of d-spacing and cell volume with composition.

3.2 Microstructural studies

Figure 2(a)-(c) reveal the scanning electron microscopic images of BZT, BZGT1, BZGT2 samples. The non-uniform distributions of the irregular shaped grains are observed in all the ceramics. The microstructural modifications in terms of grain size can be seen in the pictures. The average grain sizes were decreased sharply with Gd addition accompanied with uniform grains. As significant from the figures the average grain size for BZT is ~20µm whereas for BGZT1 and BGZT2 it reduces to ~2µm. However, no remarkable change in the density of the ceramics with the variation of Gd concentration in the BZT system. The compositional characterization was done by Energy dispersive X-ray spectroscopy (EDX) which is shown in inset of figure 2. Table 1 shows the calculated and EDX derived composition of BZT, BGZT1 and BGZT2 ceramics. There exists small variation in both the data which is possibly due the deficiency of oxygen during sintering at high temperature.

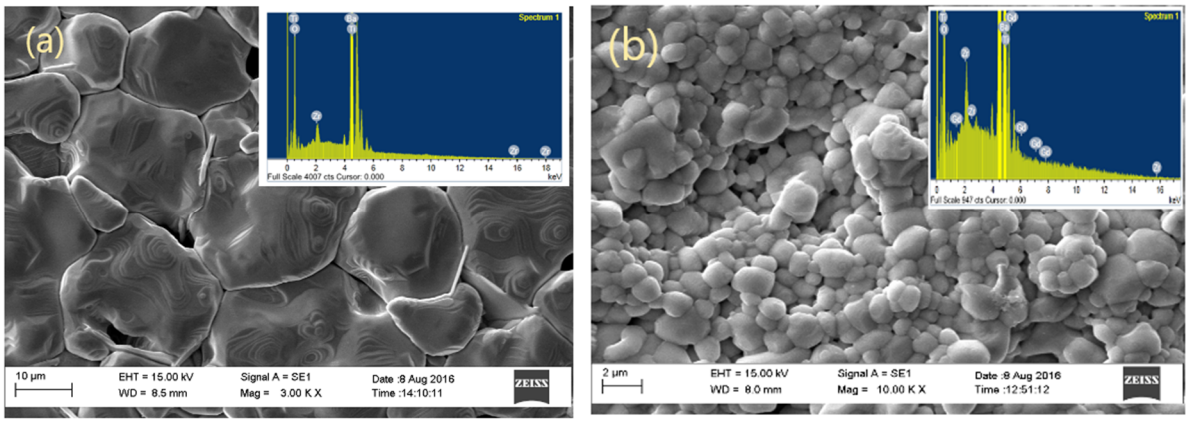

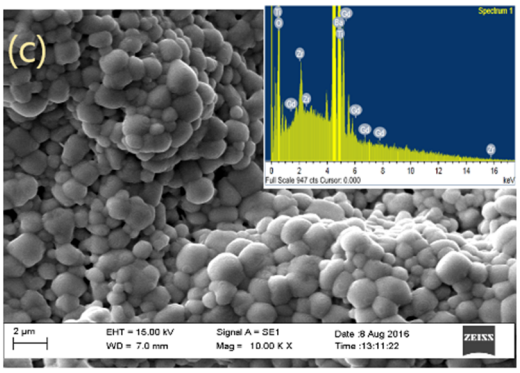

Figure 2. SEM micrographs of (a) BZT (b) BGZT1 (c) BGZT2 ceramics. The insets show EDX spectrum showing the elemental composition of the ceramics.

Table 1. Calculated and EDX derived composition of $BaGdZr_{0.05}Ti_{0.95}O_3$ ceramic.

Element	BZT		BGZT1		BGZT2	
	Wt.% calculated	Wt.% from EDX	Wt.% calculated	Wt.% from EDX	Wt.% calculated	Wt.% from EDX
Ba	57.59	57.65	56.39	56.45	56.17	56.11
Zr	1.48	1.59	1.50	1.55	1.52	1.46
Ti	18.52	18.12	18.57	18.55	18.60	18.46
O	22.41	22.64	22.96	22.85	22.90	23.12
Gd	-	-	0.58	0.60	0.81	0.85

3.3 Dielectric studies

We have done the dielectric studies and dielectric loss studies of Gd doped BZT as a function of temperature at various frequencies. But these results were reported in our earlier publication [34] so here, we only report the dielectric study as function of frequency at various temperatures. Figure 3 (a-c) illustrated the frequency dependent dielectric studies of BZT, BGZT1 and BGZT2 ceramics at various temperatures from room temperature to temperature above phase transition. We have noticed an inverse relation between dielectric constant and frequency i.e. ε' decreases with increasing frequency. All the ferroelectric materials follow this behaviour. At lower frequencies the values of dielectric constant are higher while in the higher frequency region the dielectric constant drops and attains a saturation. To understand this behaviour Debye gave a modified law for the dipoles oscillating in AC fields [35]:

$$\varepsilon^* = \varepsilon_\infty + \frac{\varepsilon_s - \varepsilon_\infty}{[1+(i\omega\tau)^{1-\alpha}]} \quad (1)$$

where ε_s and ε_∞ are the low and high-frequency values of ε, ω (=2π*f*) is the cyclic frequency, *f* is the frequency of measurement, τ is the relaxation time and α measures the distribution of relaxation time. According to this relation at lower frequencies the relaxation time is quite high so the dipoles get sufficient time to follow the electric field resulting in high value of ε'. With increasing frequency, the dipoles begin to lag behind the field as a result of which decrease in ε' values are seen. At much higher frequencies due very short relaxation times the dipoles could not orient themselves in the direction of the applied electric filed and hence reduction in the dielectric values are seen.

The inset in figure 3 shows the dielectric loss as function of frequency for the samples. The dielectric loss of the samples is less than 0.2 and for BZT and BGZT2 the value is even less than 0.1 which show good thermal stability for practical applications. The dielectric loss is attributed to the presence of oxygen vacancies which are commonly seen in the oxide perovskites. The dielectric loss curves follow the similar trend as seen in the dielectric constant vs. frequency plots. The curves are more dominant at

lower frequencies than higher frequencies. At higher frequencies the dipoles could not follow the applied AC fields because of infinitesimally small relaxation time. In BZT at some frequencies between 10^2-10^4 Hz a small hump is seen indicating dielectric relaxation in the sample however, in BGZT1 and BGZT2 samples this kind of relaxation is not seen.

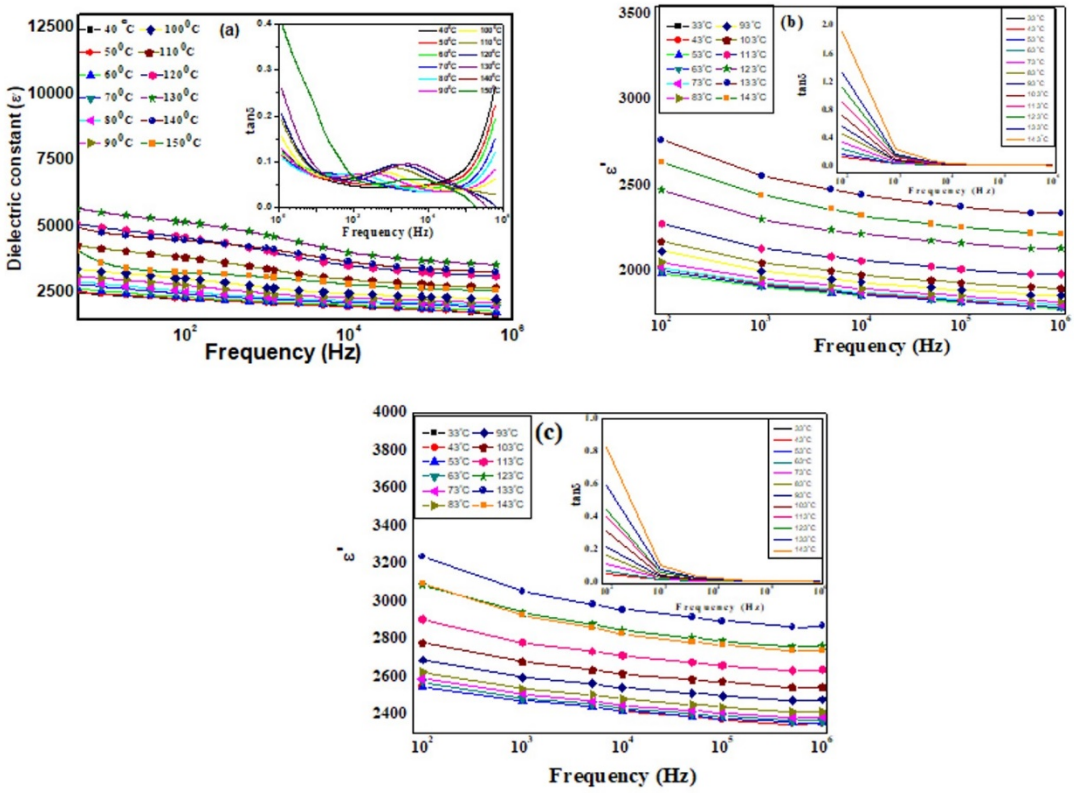

Figure 3. Variation of dielectric constant with frequency at various temperatures from room temperature to Tc. The inset shows the corresponding dielectric loss values. (a) BZT (b) BGZT1 (c) BGZT2.

The capacitance and dissipation factor of ceramic capacitors are significantly affected by doping concentrations. The permittivity/capacitance of ferroelectrics is generally temperature dependent and varies especially near to the Curie temperature. In order to measure the degree of capacitance variation with temperature, the temperature coefficients of capacitance (TCC) near phase transition temperature were calculated using the formula [36]:

$$TCC(\%)=\frac{C(T)-C(T_c)}{C(T_c)}x100\% \quad (2)$$

Where C(T) is capacitance at the temperature T and C(Tc) the reference value of the capacitance at phase transition temperature (Tc). The TCC(%) measured at 100kHz frequency is represented as a function of the temperature for BZT, BGZT1 and BGZT2 in figure 4. In case of doped samples, the variation of capacitance is less than 25% from 40°C-160°C. The corresponding temperature interval of 120°C is considered as a ceramic with good stability which is a fundamental property of all devices for energy storage application. Analysis of the plots suggests that the TCC of BGZT2 sample is almost close to the temperature stability specifications for X8R and X9R capacitors, which state that the capacitance change should fit within ±15% of the tolerance limit for long temperature range.

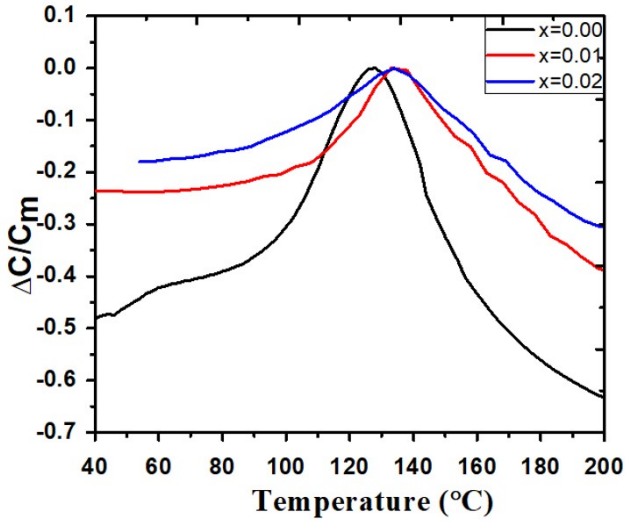

Figure 4. Temperature coefficient of capacitance with temperature.

3.4 Conductivity studies

Figure 5 shows the variation of AC conductivity of BZT, BGZT1 and BGZT2 samples with temperature (40℃-160℃ that corresponds to the temperature nearby phase transition) measured at 100kHz. Here, ac conductivity was evaluated from dielectric data by employing the following relation [37]:

$$\sigma_{ac} = \omega\varepsilon_0\varepsilon' \tan(\delta) \quad (3)$$

where, σ_{ac} is the ac conductivity, ω =2πf, is the angular frequency and ε_0 is the absolute permittivity. It isapparent from the figure that in low temperature regime the ac conductivity
depends significantly on the frequency. However, the increase in temperature, where marked dielectric relaxation takes place, reduced gradually the frequency dependence of σ_{ac}so that the conductivity was mainly determined by temperature. At still higher temperatures (near phase transition) there was a deviation probably due to the onset of dielectric phase transition. The ac conductivity found to increase with temperature at lower frequencies however, at higher frequency we could not find much variation ac conductivity. Near Curie temperature, the domain structure breaks up, carriers become free and take part in conduction mechanism. Interpretation of different theoretical models concludes that ac conductivity originates from migration of ions by hopping between neighbouring potential wells at lower temperatures which eventually give rise to dc conductivity at high temperatures. Oxygen vacancies are the most mobile charge carriers in oxide ferroelectrics and play an important role in the conduction process in most dielectric ceramics. Around the oxygen vacancy, long range potential wells may be formed, there can be large number of titanium centres within each potential well surrounding the oxygen vacancy. Conduction electrons created by the ionization of oxygen vacancies can cause hopping of electrons between Ti^{4+} and Ti^{3+} [38-40]. The figure also indicates that the introduction of Gd^{3+} ions has slightly increased the conductivity probably due to the presence of oxygen vacancies.

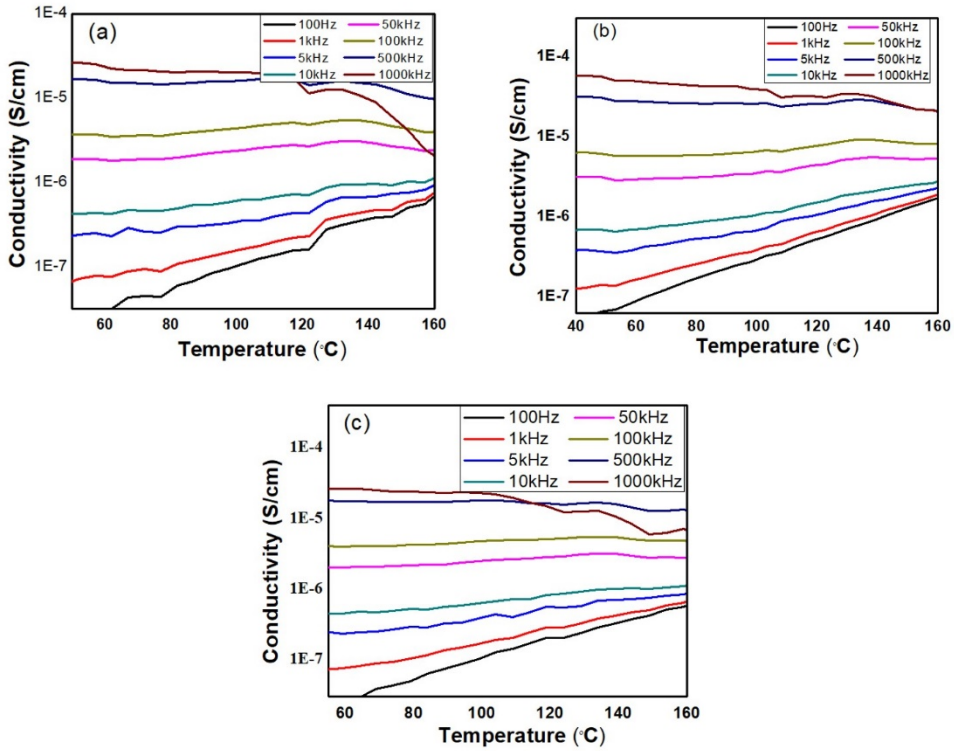

Figure 5. AC conductivity as function of temperature at various frequencies from 100Hz-1000kHz (a) BZT (b) BGZT1 (c) BGZT2.

4. Conclusion

The performance characteristics of ceramic capacitators are greatly determined by the properties of the dielectric material. Thus, from the present study we conclude that lead free ceramic samples of Gadolinium doped Barium Zirconium Titanate samples have been synthesized successfully by the conventional solid-state reaction method. The XRD technique has confirmed the perovskite phase with orthorhombic structure for BZT and tetragonal for BGZT1 and BGZT2. The microstructural studies reveal that the shape, size and distribution of BZT has got modified by addition of Gd_2O_3 in it and reduced from 20µm to 2µm. The dielectric values found to decrease for the doped samples but the dielectric loss for these samples is little larger. Also, the variations in temperature effected capacitance and dissipation factor of ceramic capacitors are found. The conductivity values are increased for doped samples.

References

[1] Jiang B, Iocozzia J, Zhao L, Zhang H, Harn Y W, Chen Y and Lin Z 2019 *Chemical Society Reviews* **48** 1194
[2] Bisen S, Mishra A and Jarabana K M 2016 In *AIP Conference Proceedings* (Vol. 1731, No. 1, p. 050070). AIP Publishing LLC
[3] Sidorkin A, Nesterenko L, Gagou Y, Saint-Gregoire P, Vorotnikov E and Popravko N 2018 *Materials* **11** 1436
[4] Acosta M, Novak N, Rojas V, Patel S, Vaish R, Koruza, J, Rossetti Jr.G A and Rödel J 2017 *Applied Physics Reviews* **4** 041305
[5] Li Y J, Xu M, Feng J Q and Dang Z M 2006 *Applied Physics Letters* **89** 072902
[6] Kuo D H, Chang C C, Su T Y, Wang W K and Lin B Y2001 *J. Eur. Ceram. Soc.* **21** 1171
[7] Kour P and Sinha S 2012 *Digest Journal of Nanomaterials and Biostructures* **7** 1327

[8] Bochenek D, Niemiec P and Dercz G 2020 *Materials* **13** 1996
[9] Pérez de la Cruz J, Joanni E, Vilarinho P M and KholkinA L 2010 *J. Appl. Phys.* **108**114106
[10] Gupta R, Verma S, Singh V and Bamzai K K 2015 Processing and Application of Ceramics **9** 1
[11] Zhan X L, Chen Z X, Cross L E and Schulze WA 1983 *J. Mat. Sci.* **18** 968
[12] Zhang Q M, Zhao J and Cross L E 1996 *J. appl.Phys.* **79** 3181
[13] Lü C, Zhang Y, Zhang H, Zhang Z, Shen M and Chen Y 2019 *Energy Conversion and Management* **182** 34
[14] Ahmad M M, Alismail L, Alshoaibi A, Aljaafari A, Kotb H M and Hassanie R 2019 *Results in Phys.* **15** 102799
[15] Kuang S J, Tang X G, Li L Y, Jiang Y P and Liu Q X 2009 *Scripta Materialia* **61** 68
[16] Puli V S, Pradhan D K, Riggs B C, Chrisey D B andKatiyar R S 2014 *J. alloys and compds.* **584** 369
[17] Thanachayanont C, Yordsri V, Kijamnajsuk S, Binhayeeniyi N and Muensit N 2012 *Materials Lett.* **82** 205
[18] Xue D, Gao J, Zhou Y, Ding X and Ren X 2015 *J. Appl. Phys.* **117** 124107
[19] Park I J, and Han Y H 2014 *Metals and Mater. Inter.* **20** 1157
[20] Narang S B and Kaur D. 2009 *Int.Ferroelectr.* **105** 87
[21] Hernández LaraJ P, Pérez Labra M, Barrientos Hernández F R, Romero Serrano JA, Ávila Dávila O, Thangarasu P, and Hernández Ramirez A 2017 *Mater.Resrch.* **20** 538
[22] Huang X, Zhang W, Xie J, Xu Q, Zhang L, Hao H, and Cao M 2017 *J. Mater. Sci.: Mater. in Electr.* **28** 4204
[23] Billah M, Ahamed A A, Sen A and Rahman M M 2015 International Conference on Mechanical, Industrial and Materials Engineering, ICMIME 2015
[24] Karuppanan A, Athikesavan V, Bhargav P B and Ramasamy P 2020 *J. Mater. Sci.: Mater. in Electr.* **1**10
[25] Canu G, Bottaro G, Buscaglia M T, Costa C, Condurache O, Curecheriu L and Armelao L 2019 *Sci. reports*. **9** 1
[26] Zhang Q, Chen J and Che M 2020 *Ferroelectrics*. **566** 30
[27] Moura F, Simões A Z, Stojanovic B D, Zaghete M A, Longo E and Varela J A 2008 *J. Alloys and Compds.* **462** 129
[28] Mahesh M L V, Prasad V B and James A R 2013 J. Mater. Sci.: Mater. Electron. **24** 4684
[29] Muensita S and Binhayeeniyi N 2010 In 2010 3rd International Nanoelectronics Conference (INEC) (p 877-877). IEEE.
[30] Garbarz-Glos B, Bormanis, K, Kalvane A, Jankowska-Sumara I, Budziak A, Suchanicz W and Śmiga W 2011 *Int. Ferroelectrics*, **123** 130
[31] Borah M and Mohanta D 2014 Appl. Phys. A. **115** 1057
[32] Li L, Wang M, Guo D, Fu R and Meng Q 2013 *J. Electroceram.* **30** 129
[33] Reddy S B, Rao K P and Rao M R 2011 *J. alloys and compds.* **509** 1266
[34] Bhargavi G N, Khare A, Badapanda T and Anwar M S 2018 *Appl. Phys. A* **124** 746
[35] Wilson J N, Frost J M, Wallace S K and Walsh A 2019 *APL Materials* **7** 010901
[36] Borderon C, Nadaud K, Coulibaly M, Renoud R and Gundel H 2019 *Int. J. Adv. Resrch. Phys. Sci.* **6** 2349
[37] Reddy P S and Rao TS 2014 *Int. J. Eng. Resrch. & Tech.* **3** 857
[38] Funke K 1993 *Porgs. Sol. Stat. Chem.* **22** 111
[39] Jonscher A K 1996 Universal Relaxation Law, *Chelsea Dielectrics Press Ltd*, London, ISBN 0950871125
[40] Ngai K L 1993 *Phys. Rev. B* **48** 13481

International Kindle Paperwhite

Dr. Rashmi Kujur

The Hill Korwa and Birhor

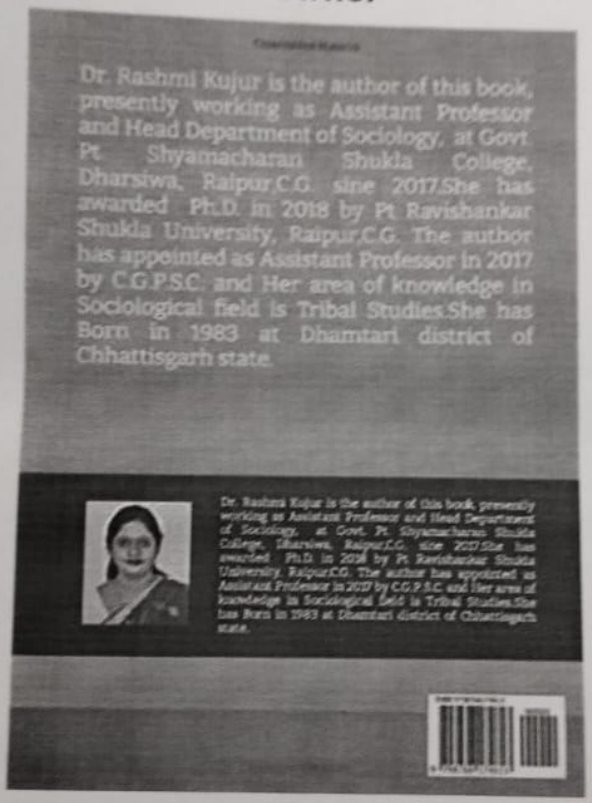

Kindle	Paperback
$3.35	$5.00

Shop all formats

ISBN : 978-93-92568-19-0

रायपुर जिले में भारत छोड़ो आन्दोलन का इतिहास

डॉ. शबनूर सिद्दीकी

डॉ. शबनूर सिद्दीकी

जन्म : रायपुर छत्तीसगढ़

शिक्षा : एम.ए. इतिहास, प्रवीण्य सूची में छठवा स्थान, पी.एच.डी. 1997। अनेक शोध पत्रिका में शोध पत्र एवं आलेख प्रकाशित। अनेक रचनाए एवं ऐतिहासिक आलेख समाचार पत्रों में प्रकाशित।

पंडित रविशंकर शुक्ल केन्द्रीय समिति, पाठ्यक्रम संबंधी इतिहास विषय विशेषज्ञ।

चैक–चौराहो पर महापुरुषो की मूर्ति स्थापना–सदस्य।

संप्रति : विभागाध्यक्ष एवं प्राध्यापक इतिहास
शासकीय पंडित श्यामाचरण शुक्ल महाविद्यालय, धरसींवा (छ.ग), वर्तमान में प्रभारी प्राचार्य, शासकीय पंडित श्यामाचरण शुक्ल महाविद्यालय, धरसीवा (छ.ग.)

Aditi Publication
OPP. NEW PANCHJANYA VIDYA MANDIR,
NEAR TIRANGA CHOWK, KUSHALPUR, DIST-
RAIPUR-492001, CHHATTISGARH
shodhsamagam1@gmail.com
+91 9425210308

9 789392 508190
₹ 349

रायपुर जिले में भारत छोड़ो आन्दोलन का इतिहास

2022
Edition - **01**

लेखक
डॉ. शबनूर सिद्दीकी,
प्रध्यापक, इतिहास,
शासकीय पं. श्यामाचरण शुक्ल महाविद्यालय,
धरसींवा, छत्तीसगढ़

ISBN : **978-93-92568-19-0**

Price : Rs. **349/-**

Publisher & Prnted by:
Aditi Publication,
Opp. New Panchajanya vidya Mandir, Near Tiranga Chowk,
Kushalpur, Raipur, Chhattisgarh, INDIA
+91 9425210308